FREE VIBRATION ANALYSIS OF TRUSSES APPLYING THE GENERALIZED FINITE ELEMENT METHOD WITH A SELECTIVE MESH ENRICHMENT

Maicon Felipe Malacarne

Marcos Arndt

Roberto Dalledone Machado

Paulo de Oliveira Weinhardt

maicon.unicentro@hotmail.com

arndt.marcos@gmail.com

roberto.dalledonemachado@gmail.com

paulo.weinhardt@yahoo.com.br

Universidade Federal do Paraná- UFPR
Jardim das Américas, CEP: 81531-990 - Curitiba, PR – Brasil

Abstract. *This work consists in propose a selective mesh enrichment using the Generalized Finite Element Method (GFEM) applied to free vibration analysis of trusses. For this, the Friberg Indicator is used, because it has the property of identify which elements present a greater contribution in the convergence of the approximation when applying the GFEM from an initial solution obtained by the Finite Element Method (FEM). As the enrichment with GFEM is performed, the mass and stiffness matrices have their dimensions increased in a significant way. By identifying the elements that better influence the convergence of the approximation, it is possible to enrich only these elements, thus solving a system of smaller size, with an error close to the error obtained with the enrichment of all elements of the mesh.*

Keywords: *GFEM, Trusses, Friberg Indicator, Selective Mesh Enrichment.*

INTRODUCTION

When an approximate solution of a boundary value problem is obtained, it is of utmost importance to know how far the approximation lies from the analytical solution. As introduced by Petroli (2016), usually in engineering problems, it is not possible to get the exact solution, so the approximate methods are the only way out.

In this perspective, the GFEM is presented as a tool to obtain an approximate solution for different boundary value problems and a current research topic addressed in different problems, some of them described by: Weinhardt (2016), Petroli (2016), Torres, Barcellos and Barros (2016), Ferreira, Barros and Greco (2016), Mendonça, Chamoin and Barcellos (2016), Shang (2014), Torii (2012), Arndt (2009) and others.

The error indicator proposed by Friberg (1986) and also discussed by Friberg and Moller (1987) can be used to estimate the relative error related to a target frequency in a free vibration analysis, when we wish to improve an initial FEM solution by an increase in the number of degrees of freedom.

In this work the Friberg indicator is applied in GFEM dynamic analysis of trusses in order to identify which elements in the mesh may be enriched to better improve the precision of a chosen frequency. The proposed selective GFEM mesh enrichment can reduce the computational cost of the dynamic analysis.

2 GENERALIZED FINITE ELEMENT METHOD

According Góis and Proença (2008) the Generalized Finite Element Method (GFEM) is characterized as an unconventional extension of the Finite Element Method, because the GFEM incorporates characteristics and techniques of the Meshless Methods, such as nodal enrichment. This method is used to solve boundary value problems, which consists of a differential equation that governs a given problem, along with the boundary conditions, which may be Neumann or Dirichlet conditions.

According to Torii (2012), the GFEM allows the inclusion of non-polynomial functions (commonly trigonometric) in the approximation space. The studied phenomena generally have known characteristics those allow to select non-polynomial functions in order of better represent the phenomenon. This approach can generate a significant improvement in the convergence of the approximation, since the approximation space of the functions tends to better describe the exact solution space of the problem.

Another important property for the GFEM, which brings advantages to the dynamic analysis of structures, is the fact that it meets the criteria of the Unit Partition (PU), as shown by Melenk and Babuska (1996). The space obtained with the PU inherits properties of conformity and regularity of the original space, where the new function space has compact support and the sum of its values for the domain Ω is always unitary.

The GFEM has been presenting excellent results for problems as dynamic analysis of bars, beams, trusses and frames, crack analysis, plasticity, two-dimensional wave equation, plane stress state and others. In dynamic analysis, as presented by Weinhardt (2016), the approximations obtained by FEM present difficulties and limitations in obtaining higher frequencies and the use of GFEM becomes attractive in these cases, since this one presents good results especially in the determination of high frequencies.

In GFEM trigonometric functions can be constructed starting from the fundamental relation $\sin^2 x + \cos^2 x = 1$ for all x belonging to the real. Thus for a finite element of local coordinates ξ = [0,1], the following functions can be defined:

$$\phi_1^e = \cos^2\ (\xi.\frac{\pi}{2}) \quad (1)$$

$$\phi_2^e = \sin^2\ (\xi.\frac{\pi}{2}) \quad (2)$$

Where the functions presented by Eq. (1) and Eq. (2) are examples of functions that can be used in the PU so that its properties are satisfied. In this way there is no interference of the elementary functions in the global domain, since the union between the elements respects the completeness and compliance criteria. The above functions are represented graphically by Fig. 1.

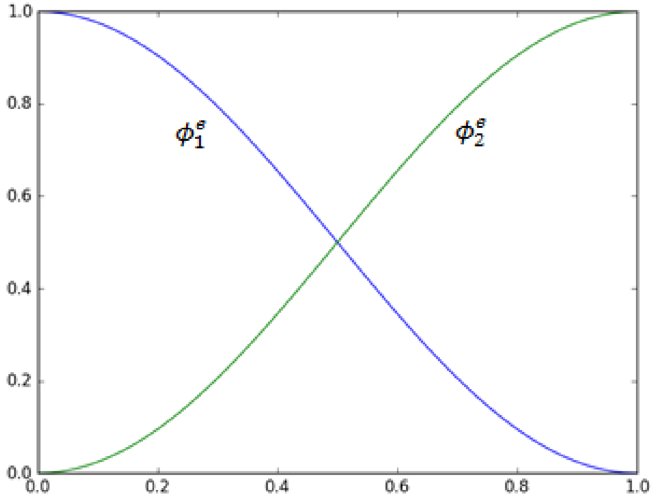

Figure 1. Functions that meet the PU standard.

As already mentioned, one of the GFEM applications is the free vibration of a bar, considering only axial displacement, as illustrated in Fig. 2.

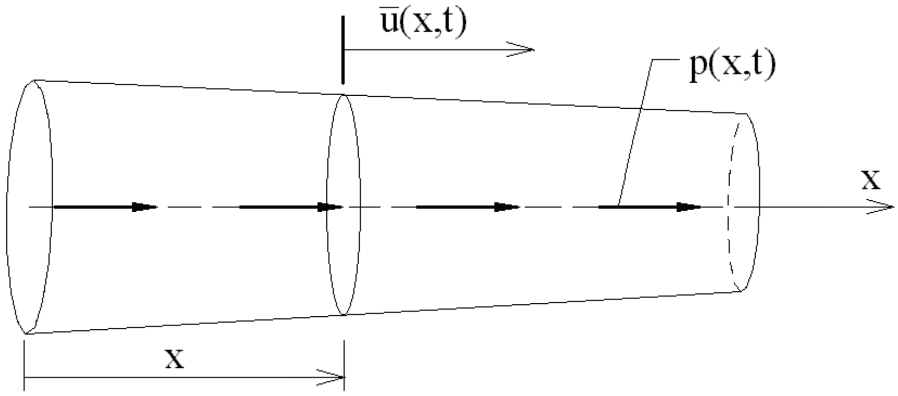

Figure 2.Straight bar with axial deformation.
Arndt (2009)

The partial differential equation describing the free vibration of a uniform bar is:

$$\rho \frac{\partial^2 \bar{u}}{\partial t^2} - E \frac{\partial^2 \bar{u}}{\partial x^2} = 0 \tag{3}$$

where ρ is the specific mass, E is the modulus of elasticity, t is time, x is section position and $\bar{u}(x,t)$ is the displacement. Assuming $\bar{u}(x,t) = u(x).T(t)$, the analytical solution is given by:

$$u(x) = a.\sin(kx) + b.\cos(kx) \tag{4}$$

$$T(t) = c.\sin(\omega x) + d.\cos(\omega x) \tag{5}$$

where a, b, c and d are constants, ω is the natural vibration frequency of the bar, k is the bar wave number, and $k > 0$. Since analytical solution of the bar problem admits trigonometric terms, it is reasonable to assume approximation functions that also contain trigonometric terms, so the approximate solution tends to approximate the analytical one. In this context, the enriching functions, written in the local coordinates $\xi = [0,1]$ (Arndt , 2009):

$$\phi_3^j = \sin\ (\beta_j.L_e.\xi) \tag{6}$$

$$\phi_4^j = \left(\cos\ (\beta_j.L_e.\xi\right) - 1) \tag{7}$$

$$\phi_5^j = \sin\ (\beta_j.L_e.(\xi - 1)) \tag{8}$$

$$\phi_6^j = \left(\cos\ (\beta_j.L_e\,.(\xi - 1)\right) - 1) \tag{9}$$

are used for the simulations carried out in this work.

In Equations (6) to (9), L_e is the length of the element and β_j is a parameter such that $\beta_j = j\pi$. The functions of Eq. (6) to Eq. (9) are shown graphically in Fig. 3.

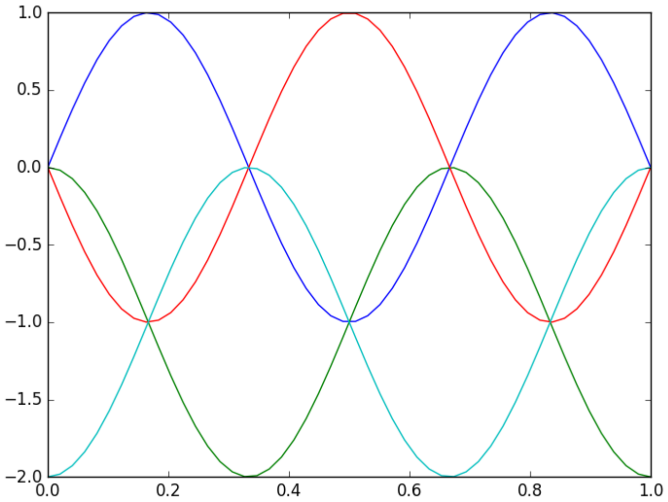

Figure 3. Enriching Functions for $\beta = 3\pi$.

3 FRIBERG INDICATOR

The Friberg error indicator was proposed by Friberg (1986), and it has the objective of predicting variations in a given eigenvalue caused by the addition of new polynomials with greater degree in the approximation space, when the *p*-hierarchical Finite Element Method is implemented. This indicator is not an approximation of the error, but it is a dimensionless value that allows comparisons between possible variations of an eigenvalue when different functions are added in the process of obtaining a specific natural frequency of the structure.

The boundary value problem related to the non-damped free vibration problem is given by (Soriano, 2014):

$$[M].\{\ddot{u}\} + [K].\{u\} = 0 \tag{10}$$

where $[M]$ is the mass matrix, $\{\ddot{u}\}$ is the acceleration vector, $[K]$ is the stiffness matrix and $\{u\}$ is the vector of the displacements. Assuming harmonic displacements, the Eq. (10) becomes a generalized eigenvalue problem as described in detail by Carey and Oden (1984). After an initial approximation obtained by the FEM for a dimension system nxn, if a GFEM analysis is performed one obtains a new approximation for a system of dimension $n+m$, whose block matrix representation is given by:

$$\left(\begin{bmatrix}[K]_{nxn} & [K]_{nxm}\\ [K]_{mxn} & [K]_{mxm}\end{bmatrix} - \lambda_i.\begin{bmatrix}[M]_{nxn} & [M]_{nxm}\\ [M]_{mxn} & [M]_{mxm}\end{bmatrix}\right).\begin{Bmatrix}\Phi_n\\ \Phi_m\end{Bmatrix} = 0 \tag{11}$$

where the block belonging to the FEM consists of: $[K]_{nxn}$ the stiffness matrix, $[M]_{nxn}$ the mass matrix, Φ_n the n dimension eigenvector associated to the eigenvalue λ_i. The block belonging to the GFEM is composed by: stiffness matrices $[K]_{mxn}$, $[K]_{nxm}$ and $[K]_{mxm}$, the mass matrices $[M]_{mxn}$, $[M]_{nxm}$ e $[M]_{mxm}$, and the increase in the Φ_n which is associated to λ_i is represented by Φ_m. A relative variation (η_i) is written from a Taylor series expansion and the Rayleigh quotient as:

$$\eta_i = \frac{\Delta\lambda_i}{\lambda_i} \approx A * B \tag{12}$$

where:

$$A = \{\Phi_n{}^T\}.([K]_{mxn} - \lambda_i[M]_{mxn})^T.(([K]_{mxm} - \lambda_i[M]_{mxm})^{-1})^T \tag{13}$$

$$B = \frac{([K]_{mxn} - \lambda_i.[M]_{mxn}).\{\Phi_i\}_n}{(\{\Phi_i^T\}_n.[K]_{nxn}.\{\Phi_i\}_n)} \tag{14}$$

More details are presented by Duarte (2003).

Therefore Eq. (12) allows evaluating the variation in the eigenvalue λ_i by inclusion of the GFEM enriching functions without the need to solve the matrix system presented in Eq. (11).

The relation between the natural frequency ω_i and the eigenvalue λ_i is given by:

$$\omega_i = \sqrt{\lambda_i} \tag{15}$$

Proceedings of the XXXVIII Iberian Latin-American Congress on Computational Methods in Engineering
P.O. Faria, R.H. Lopez, L.F.F. Miguel, W.J.S. Gomes, M. Noronha (Editores), ABMEC, Florianópolis, SC, Brazil, November 5-8, 2017.

Then, due to the strong relation between the eigenvalue λ_i and the frequency ω_i, the Friberg indicator η_i can be used to give an idea of the variation caused by the GFEM at a given frequency. According to Weiberg (1997), the approach applying an error indicator can be used in an iterative process to select elements of interest where the refinement better improve the results. This can be done based on the ordered values of positive maximum indicators, which represent the major changes in an eigenvalue.

4 DYNAMIC ANALYSIS OF TRUSSES

The dynamic analysis of plane trusses is based on a system formed by the union of straight bars, which are modeled by the partial differential equation given in Eq. (3), admitting only axial deformations. According to Arndt (2009), the analytical solution for the free vibration problem of trusses is rarely found in the literature, so the approximate solutions are an alternative to find the solution of these problems. Because plane trusses have non-collinear longitudinal axes, two coordinate systems, one local and the other global, are used as illustrated in Fig. 4.

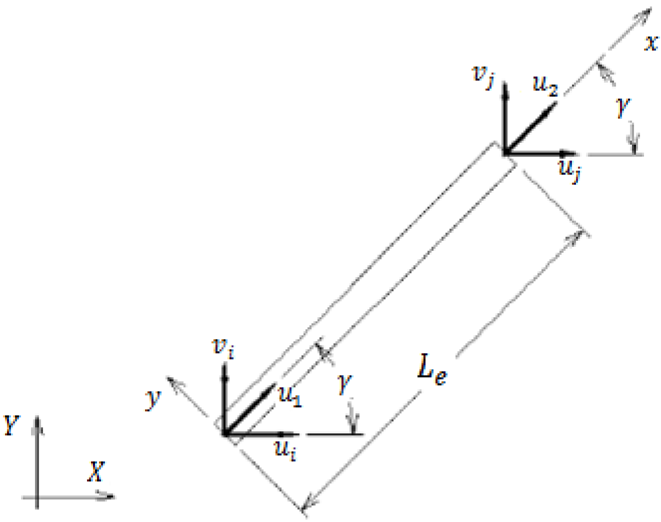

Figure 4. Local and global coordinate systems for a truss bar.
Arndt (2009).

An element with two degrees of freedom in local coordinate system becomes a four degrees of freedom element in global coordinate system. The local element degrees of freedom u can be related to the global ones U by the rotation matrix

$$T = \begin{bmatrix} \cos\gamma & \sin\gamma & 0 & 0 \\ 0 & 0 & \cos\gamma & \sin\gamma \end{bmatrix} \tag{16}$$

where γ is the angle of rotation of the element.

The rotation influences the FEM system, so that the elementary stiffness matrix is written as $[K^e] = [T]^T[K][T]$ and the elementary mass matrix is written as $[M^e] = [T]^T[M][T]$, presented by :

$$[K^e] = \frac{A.E}{L_e}\begin{bmatrix} \cos^2\gamma & \cos\gamma\,.\sin\gamma & -\cos^2\gamma & -\cos\gamma\,.\sin\gamma \\ \cos\gamma\,.\sin\gamma & \sin^2\gamma & -\cos\gamma\,.\sin\gamma & -\sin^2\gamma \\ -\cos^2\gamma & -\cos\gamma\,.\sin\gamma & \cos^2\gamma & \cos\gamma\,.\sin\gamma \\ -\cos\gamma\,.\sin\gamma & -\sin^2\gamma & \cos\gamma\,.\sin\gamma & \sin^2\gamma \end{bmatrix} \quad (17)$$

$$[M^e] = \frac{\rho.A.L_e}{3}\begin{bmatrix} \cos^2\gamma & \cos\gamma\,.\sin\gamma & \frac{1}{2}\cos^2\gamma & \frac{1}{2}\cos\gamma\,.\sin\gamma \\ \cos\gamma\,.\sin\gamma & \sin^2\gamma & \frac{1}{2}\cos\gamma\,.\sin\gamma & \frac{1}{2}\sin^2\gamma \\ \frac{1}{2}\cos^2\gamma & \frac{1}{2}\cos\gamma\,.\sin\gamma & \cos^2\gamma & \cos\gamma\,.\sin\gamma \\ \frac{1}{2}\cos\gamma\,.\sin\gamma & \frac{1}{2}\sin^2\gamma & \cos\gamma\,.\sin\gamma & \sin^2\gamma \end{bmatrix} \quad (18)$$

When GFEM enrichment functions are used new degrees of freedom are created. These new field degrees of freedom are not affected by the coordinate system change. Thus the coordinate transformation of the local displacement vector u in the global vector U is written by:

$$\begin{bmatrix} u_1 \\ u_2 \\ c_1 \\ c_2 \\ \vdots \\ c_n \end{bmatrix} = \begin{bmatrix} \cos\gamma & \sin\gamma & 0 & 0 & 0 & 0 & \dots & 0 \\ 0 & 0 & \cos\gamma & \sin\gamma & 0 & 0 & \dots & 0 \\ 0 & 0 & 0 & 0 & 1 & 0 & \dots & 0 \\ 0 & 0 & 0 & 0 & 0 & 1 & \dots & 0 \\ \vdots & \vdots & \vdots & \vdots & \vdots & \vdots & \ddots & \vdots \\ 0 & 0 & 0 & 0 & 0 & 0 & \dots & 1 \end{bmatrix} \begin{bmatrix} u_i \\ v_i \\ u_j \\ v_j \\ c_1 \\ c_2 \\ \vdots \\ c_n \end{bmatrix} \quad (19)$$

where u_1 and u_2 are the local displacements before rotation, $c_1, c_2, \dots, c_n$ are the n field degrees of freedom related to the GFEM, u_i, v_i, u_j, v_j are the global degrees of freedom in global directions X and Y.

According to Duarte, Babuska and Oden (2000), the analysis using the GFEM can significantly improve the performance of the approximation process, also making possible in some cases to obtain a more accurate approximation, which would be closer to analytical than an analysis using the FEM.

5 NUMERICAL SIMULATION

For the numerical simulation the free vibration of a seven bar truss proposed by Zeng (1998) is analyzed. The GFEM analysis was implemented in Python language version 2.7, because it is a powerful and easy manipulation tool. The geometry of the structure represented by seven elements is illustrated in Fig. 5. The characteristics of the structure are: cross-sectional area $A = 0.001\, m^2$, specific mass $\rho = 8000.0\, kg/m^3$, modulus of elasticity $E = 2.1\ 10^{11}\ N/m^2$.

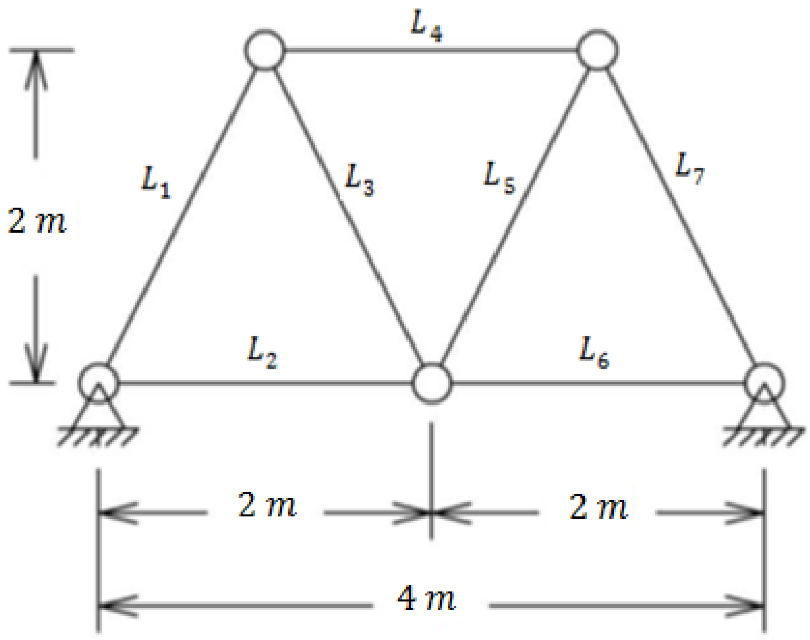

Figure 5. Seven bar truss.

The first six frequencies obtained by the linear FEM and compared FEM-p found in Cittadin (2017) with ten degree polynomial are presented in Table 1. The unit of frequencies is rad/s.

Table 1. Result FEM-linear and FEM-p.

Frequency	FEM-linear	FEM-p
ω_1	1683.5214	1647.7844
ω_2	1776.2784	1740.8397
ω_3	3341.3752	3111.3227
ω_4	5174.3538	4561.8173
ω_5	5678.1845	4823.2486
ω_6	8315.4006	7379.4823

According Carey and Oden (1984), the numerical approximation performed here is an upper-bound approximation, so smaller approximations of a frequency represents better approximations.

Then the GFEM is applied with one level of enrichment and $\beta = 1\pi$ and aiming to improve the approximations previously found by linear FEM.

But in this work the application of the GFEM is not performed in a conventional way, since a target frequency is chosen and the Friberg indicator is used to analyze the contribution in the convergence of the target frequency that each element presents when applying the enrichment functions.

To do this, the first element L_1 is enriched and the respective value of the Friberg indicator for a target frequency is calculated by Eq. (12). In order to verify if the indicator can measure the relative frequency variation, the new enriched system (Eq. (11)) is solved, finding a new approximation for the target frequency. In a practical process, the new system does not need to be solved, because the indicator here has the property of realizing a dimensionless projection of the relative variation of a certain frequency, without the new system being solved.

This process is repeated until all seven elements receive the GFEM functions, one at a time. At the end, seven values are obtained for the indicator and the comparison can be made, so that the element that presents the highest value of the indicator will be the element that contributes most to the convergence of the approximation.

5.1 Frequency $\boldsymbol{\omega_1}$

The Friberg indicators and the first frequency obtained enriching each element are presented in Table 2, recalling that the approximation found by the linear FEM was ω_1 =1683.5214.

Table 2. Results local GFEM- First frequency

Element	η_i	ω_1
L_1	0.0023	1681.5380
L_2	1.25x10^{-33}	1683.5214
$\boldsymbol{L_3}$	**0.0202**	**1666.6351**
L_4	4.69x10^{-5}	1683.4819
$\boldsymbol{L_5}$	**0.0202**	**1666.6351**
L_6	1.25x10^{-33}	1683.5214
L_7	0.0023	1681.5380

The Friberg indicator η_i shows the highest values for third and fifth elements. Analyzing the results obtained by GFEM when third or fifth element is enriched it is verified that the indicator is successful, because in these cases the approximation obtained is better than other elements.

It is also observed that elements two and six present the smallest values for the indicator η_i and have an approximation with very little difference from that found with the linear FEM. Therefore, there is no need to enrich these elements, since the contribution they make to convergence is minimal.

Is important to note that the Friberg indicator values are the same for the pairs of elements: three and five, two and six, one and seven. This is due to symmetry of the structure.

This behavior shows that Friberg indicator is reliable once it presents same values for symmetric elements.

A selective GFEM refinement can be then performed based on the results presented in Table 2. The selective GFEM is applied to the elements of the mesh respecting the descending order of the values of the indicator, that is L_3, L_5, L_1, L_7, L_4, L_2 and L_6. Each time an element receives the enriching functions, the new system is solved, thus obtaining a new approximation, in order to verify what happens with the convergence of the approximations as the enrichment happens. The GFEM results are presented in Table 3.

Table 3. Results of selective GFEM – First frequency

Element	ω_1
L_3	1666.6351
L_3, L_5	1651.7579
L_3, L_5, L_1	1650.0392
L_3, L_5, L_1, L_7	1648.3679
L_3, L_5, L_1, L_7, L_4	1647.7854
$L_3, L_5, L_1, L_7, L_4, L_2$	1647.7854
$L_3, L_5, L_1, L_7, L_2, L_6$	1647.7854

The results in Table 3 show that the approximate solution presents a greater convergence when the first five elements receive the functions of GFEM, and the approximation presents a low convergence when the others two elements are enriched. This is due to the fact that they present Friberg indicator values very small, that is, the improvement in the approximate frequency ω_1 is almost imperceptible when these two elements are enriched. The convergence of the target frequency may also be observed in the relationship between the decay of the approximate frequency and the increase in the number of degrees of freedom (ndof) shown in Fig. 6.

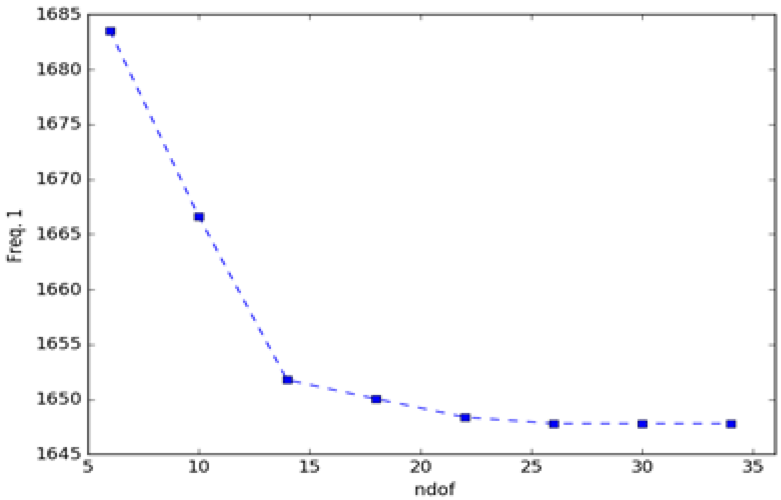

Figure 6. Relationship of first frequency decay and the number of degrees of freedom.

It is observed that the approximation of the first frequency obtained with 26 degrees of freedom is very close to that obtained with 34 degrees of freedom (all elements enriched). Even in a problem with little complexity as addressed here, the overall system can be reduced by approximately 23.6% without compromising the quality of the approach.

5.2 Frequency $\boldsymbol{\omega_2}$

The Friberg indicators and the second frequency obtained enriching each element are presented in Table 4, recalling that the approximation found by the linear FEM was $\omega_2 = 1776.2784$.

Table 4. Results of local GFEM – Second frequency

Element	η_i	ω_2
L_1	0.0015	1774.9046
L_2	0.0004	1775.8938
L_3	0.0042	1773.2236
$\boldsymbol{L_4}$	**0.0301**	**1750.8725**
L_5	0.0042	1773.2236
L_6	0.0004	1775.8939
L_7	0.0015	1774.9046

It is observed by the Friberg indicator that fourth element is the one that most influences the approximation of the second frequency when the GFEM is locally applied. Enriching this element the GFEM result for the second frequency is $\omega_2 = 1750.8725$, which is the best result among the seven elements. When enrichment functions are placed on the second or sixth element, the approximation is very close to that found with the linear FEM, that is, the variation in the target frequency is small.

Then the selective GFEM is applied again to the elements of the mesh respecting the descending order of the indicator, that in this case is L_3, L_5, L_1, L_7, L_2, L_6 and L_4. Again each one of the elements receives the enriching functions and the new system is solved to analyze the behavior of the target frequency. The selective GFEM results are presented in Fig. 7.

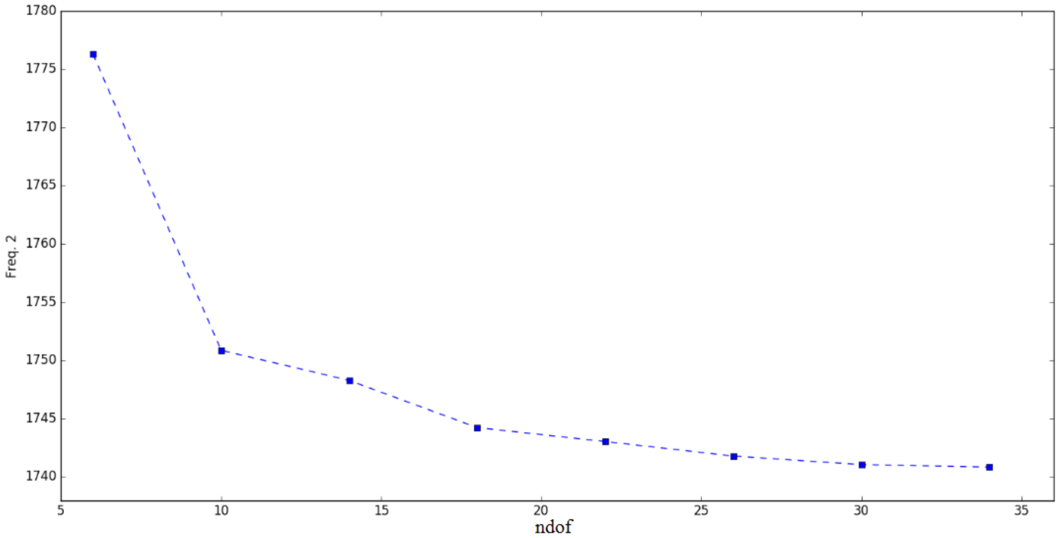

Figure 7. Relationship of second frequency decay and the number of degrees of freedom.

It is observed in Fig. 7 that the convergence is more accelerated in the elements where the value of the indicator is greater, but since the values of the indicator are relatively close for all the seven elements it is also possible to reduce the overall system size a bit without significant losing the accuracy in approach.

5.3 Frequency $\boldsymbol{\omega_3}$

The Friberg indicators and the third frequency obtained enriching each element are presented in Table 5, recalling that the approximation found by the linear FEM was ω_3 =3341.3752.

Table 5. Results of local GFEM - Third frequency

Element	η_i	ω_3
L_1	0.0320	3290.3612
L_2	0.0156	3315.3155
$\boldsymbol{L_3}$	**0.0391**	**3287.7435**
L_4	0.0062	3332.5257
$\boldsymbol{L_5}$	**0.0391**	**3287.7435**
L_6	0.0156	3315.3155
L_7	0.0320	3290.3612

The third and fifth elements are the ones that most influence the convergence of the approximation when the GFEM is locally applied, generating an approximation for the third frequency of ω_3 = 3287.7435. The fourth element is the one that presents the smallest contribution, since it has the lowest Friberg indicator value and produces the worst approximation for the third frequency.

Then the selective GFEM is applied again to the elements of the mesh respecting the the descending order of the indicator, that is L_3, L_5, L_1, L_7, L_2, L_6 and L_4. The selective GFEM results are presented in Fig. 8.

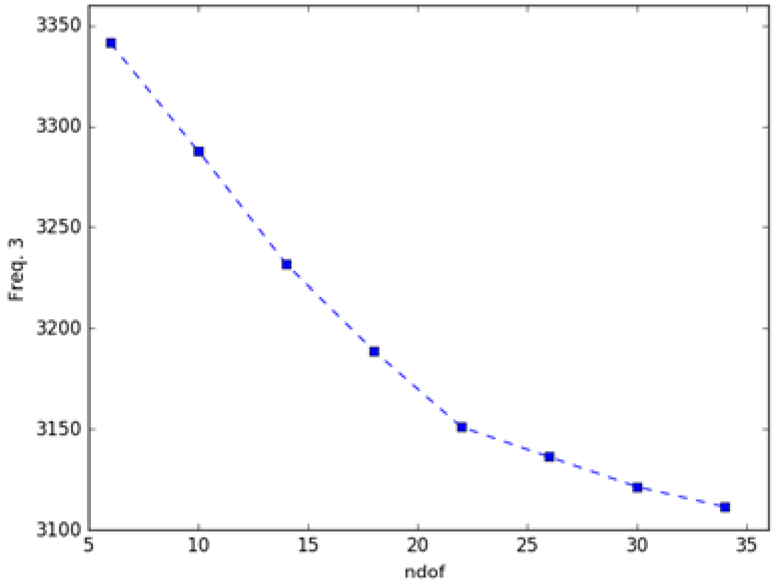

Figure 8. Relationship of third frequency decay and the number of degrees of freedom.

In this case the rate of convergence is similar when the first four elements are enriched, after which the convergence slows down, but the contribution of each element remains significant, as indicated by the values of the indicator in Table 5, so it is not possible to reduce the global system without some precision lost if the target frequency is ω_3.

5.4 Frequency ω_4

The Friberg indicators and the fourth frequency obtained enriching each element are presented in Table 6, recalling that the approximation found by the linear FEM was ω_4 =5174.3538.

Table 6. Results of local GFEM - Fourth frequency.

Element	η_i	ω_4
L_1	0.0597	4982.0062
$\boldsymbol{L_2}$	**0.1304**	**4928.2373**
L_3	0.0186	5137.2190
L_4	0.0104	5156.6270
L_5	0.0186	5137.2190
$\boldsymbol{L_6}$	**0.1304**	**4928.2373**
L_7	0.0597	4982.0062

It can be noted that second and sixth elements are the ones that most influence the convergence of the approximation when the GFEM is locally applied, generating an approximation for the fourth frequency of $\omega_4 = 4928.2373$. It is important to highlight that these elements would not have this influence if any one of the other five frequencies was adopted as the target frequency. It is also observed that the Friberg indicator perfectly shows the importance of each element in the approximation process.

Selective GFEM is applied again in the elements in order to analize the relation between convergence and the values of the indicator for this frequency. Again the enrichment order follows the decreasing order of the indicator, that is L_2, L_6, L_1, L_7, L_3, L_5 and L_4. The selective GFEM results are presented in Fig. 9.

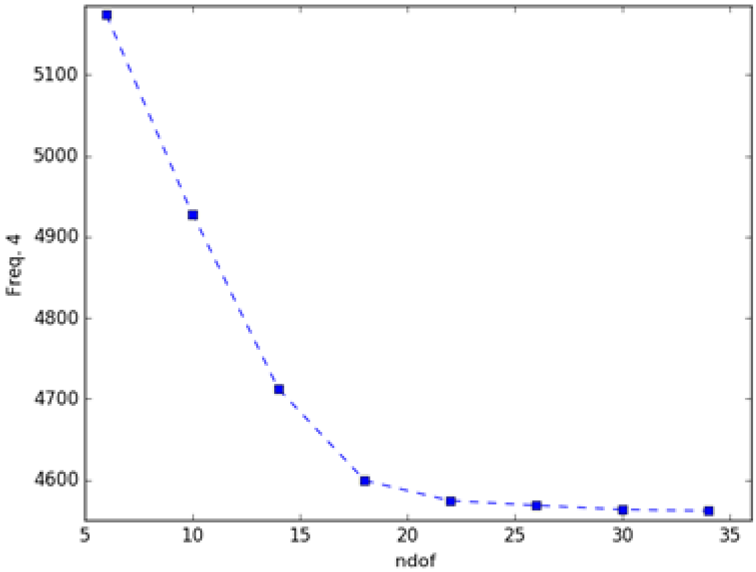

Figure 9. Relationship of the fourth frequency decay and the number of degrees of freedom.

Again the convergence is more accelerated when the elements with the highest value of the Friberg indicator are enriched and where the values are smaller the convergence is also smaller. It is observed also that the overall system can be reduced without significant losing the accuracy in approach.

5.5 Frequency ω_5

The Friberg indicators and the fifth frequency obtained enriching each element are presented in Table 7, recalling that the approximation found by the linear FEM was ω_5 =5678.1845.

Table 7. Results of local GFEM - Fifth frequency.

Element	η_i	ω_5
$\boldsymbol{L_1}$	**0.3149**	**5388.7857**
L_2	6.6x10^{-32}	5678.1845
L_3	0.0463	5601.9137
L_4	0.0130	5640.8627
L_5	0.0463	5601.9137

L_6	$6.6\text{x}10^{-32}$	5678.1845
$\boldsymbol{L_7}$	**0.3149**	**5388.7857**

The first and seventh elements are the ones that influence the convergence of the approach more when the GFEM is applied, generating an approximation for the fifth frequency of $\omega_5 = 5388.7857$.

Again the selective GFEM is applied to the elements following descending order of the indicator, that is L_1, L_7, L_3, L_5, L_4, L_2 e L_5. The convergence of the selective GFEM approximation with respect to the increase in the number of degrees of freedom can be observed in Fig. 10.

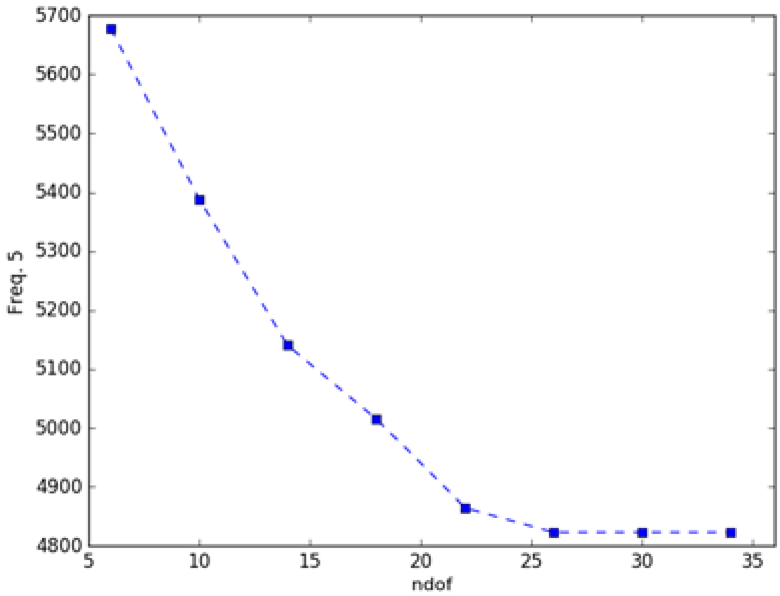

Figure 10. Relationship of fifth frequency decay and the number of degrees of freedom.

When the second and sixth elements are enriched the change in target frequency are insignificant as indicated by the extremely small value of the Friberg indicator . This means that these elements do not need to be enriched, as their contribution is insignificant for the convergence of the approach. Therefore, for this frequency, only 28 degrees of freedom are required to obtain the target frequency, i.e. there is a reduction of approximately 23.6% in the overall system size over the conventional GFEM system (all elements enriched).

5.6 Frequency $\boldsymbol{\omega_6}$

The Friberg indicators and the sixth frequency obtained enriching each element are presented in Table 8, recalling that the approximation found by the linear FEM was $\omega_6 = 8315.4006$.

Table 8. Results of local GFEM - Sixth frequency.

Element	η_i	ω_6

Proceedings of the XXXVIII Iberian Latin-American Congress on Computational Methods in Engineering
P.O. Faria, R.H. Lopez, L.F.F. Miguel, W.J.S. Gomes, M. Noronha (Editores), ABMEC, Florianópolis, SC, Brazil, November 5-8, 2017.

L_1	0.0090	8291.1893
L_2	$3.9\text{x}10^{-33}$	8315.4006
L_3	0.0896	8015.9134
$\boldsymbol{L_4}$	**0.0986**	**7988.4655**
L_5	0.0896	8015.9134
L_6	$3.9\text{x}10^{-33}$	8315.4006
L_7	0.0090	8291.1893

The fourth element is the one that most influences the convergence of the approximation when the GFEM is locally applied, generating an approximation for the sixth frequency of $\omega_6 =$ 7988.4655. However the third and fifth elements have Friberg indicator values close to the fourth element. This means that the contribution of these three elements is similar, fact proven when each local system is solved, once the obtained approximations for ω_6 are relatively close.

Then the selective GFEM is applied to the elements following the descending order of the indicator, that is L_4, L_3, L_5, L_1, L_7, L_2 and L_6. The selective GFEM results are presented in Fig. 11.

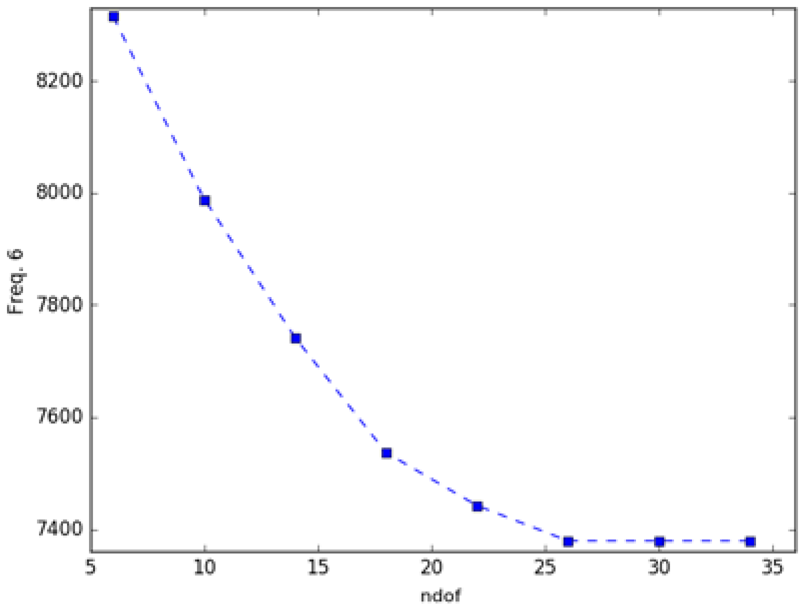

Figure 11. Relationship of sixth frequency decay and the number of degrees of freedom.

The second and sixth elements have very small Friberg indicator values similar to those found for the first and fifth frequencies, so for this target frequency they do not need to be enriched. It is observed also that the overall system can be reduced without significant accuracy losing in approach.

6 CONCLUSION

The numerical simulation presented in this work demonstrated the efficiency of the Friberg indicator to predict variations in the frequencies caused by the addition of new degrees of freedom from the application of GFEM in the problem of free vibration of a plane truss. It is noteworthy that when the target frequency was changed, the indicator pointed out the elements that contribute more to that frequency, so different strategies can be implemented to find the superconvergent elements in each analysis.

One of the contributions of the use of the Friberg indicator combined with the GFEM is the possibility of choosing one of the frequencies as the target frequency and since the indicator can predict which are the most important elements for approaching the chosen frequency, it is possible to select mesh regions to enrich instead of enrich all the mesh. In real problems where there is a high number of degrees of freedom, the use of the proposed procedure can reduce the number of degrees of freedom involved without significant accuracy losing and consequently reduce the computational cost in solving the generalized eigenvalue problem. A procedure to decrease the size of the systems involved is interesting, because as numerical instability increases when increases the number of degrees of freedom to numerically solve the problem.

Future works will analyze the combination of Friberg indicator and different levels of GFEM enrichment. It will be also investigated the use of this error indicator in the Adaptive GFEM.

ACKNOWLEDGEMENTS

The authors gratefully acknowledge the Postgraduate Program in Numerical Methods in Engineering - PPGMNE of the Federal University of Paraná and the Coordination for the Improvement of Higher Education Personnel (Capes).

REFERENCES

Arndt M., 2009. O Método dos Elementos Finitos Generalizado Aplicado à Análise de Vibrações Livres de Estruturas Reticuladas. Doctoral thesis, Universidade Federal do Paraná, Curitiba.

Carey, G. F., Oden J. T., 1984. Finite elements. v.2: A second course. New Jersey: Prentice-Hall.

Cattadin, C. C., 2017. Refinamento p do método dos Elementos Finitos para análise de vibração de treliças. Relatório de iniciação científica PIBIC, Universidade Federal do Paraná, Curitiba.

Duarte, C. A., Babuska I., Oden J. T., 2000. Generalized finite methods for tree-dimensional structural mechanics problems. *Computers & Structures, Elsevier*. Vol. 77, Issue 2, P. 215-232.

Duarte, H.V., 2003. Estimador de Erro para a Formulação p do Método dos Elementos Finitos Aplicado ao Problema Fluido-Estrutura, *Doctoral thesis,* Universidade Estadual de Campinas, Campinas.

Ferreira, I. P., Barros F. B., Greco, M., 2016. Estimadores de erro baseados no subdomínio e no elemento para o MEFG aplicado à análise não linear de estruturas de concreto. XXXVII Iberian Latin American Congress on Computational Methods in Engineering. Brasília.

Friberg, P. O., 1986. An error Indicator for the generalized eigenvalue problem using the hierarchical Finite Element Method. *International Journal for Numerical Methods in Engeneering*, vol. 23, pp. 91-98. 1986.

Friberg, P. O., P. Moller, 1987. An adaptive procedure for eigenvalue problems using the hierarchical Finite Element Method. *International Journal for Numerical Methods in Engeneering*, vol. 24, pp. 319-335, 1987.

Góis, W., Proença S. P. B., 2008. Método dos Elementos Finitos Generalizados em Formulação Variacional Mista. *Cadernos de Engenharia de Estruturas*, Vol. 10, n. 43, p. 1-32. São Carlos.

Melenk, J., Babuska, I., 1996. The Partition of Unity Finite Element Method: Basic Theory and Applications. *Austin: Institute for Computational Engineering and Sciences*, University of Texas at Austin, 32p. technical report.

Mendonça, P. T. R., Chamoin, L., Barcellos, C. S., 2016. Errors in quantities of interest in the Laminated Plate Bending Problem Using Hierarchic Sets of Basis Functions in GFEM. XXXVII Iberian Latin American Congress on Computational Methods in Engineering. Brasília.

Soriano, H. U., 2014. Introdução à Dinâmica das estruturas. 1 ed., Vol.1, *Elsevier*, Rio de Janeiro.

Petroli, T., 2016. Condicionamento do problema de autovalores obtido do Método dos Elementos Finitos Generalizados na Dinâmica de Estruturas. Master's thesis, Universidade Federal do Paraná, Curitiba.

Shang, Y. H., 2014. Análise Dinâmica Elastoplástica de Problemas da Mecânica de Sólidos via Métodos Enriquecidos de Elementos Finitos. Doctoral thesis. Pontíficia Universidade Católica do Paraná, Curitiba.

Torres, D. A. F., Barcellos, C. S., Barros, F. B., 2016. On the use of a continuous Strong-form residuum field for estimation in smooth GFEM aproximations. XXXVII Iberian Latin American Congress on Computational Methods in Engineering. Brasília.

Torii, A. J. 2012. Análise Dinâmica de Estruturas com o Método dos Elementos Finitos Generalizado. Doctoral thesis, Universidade Federal do Paraná, Curitiba.

Weiberg, N. E., 1997. Superconvergent Patch Recovery- a Key to quality assessed FE solutions. *Advances in Engineering Software*, *Elsevier*. Vol. 28, Issue 2, p. 85-95.

Weinhardt, P. O., 2016. Estudo da Estabilidade do Método dos Elementos Finitos Generalizados Aplicado à Análise Dinâmica. Master's thesis. Universidade Federal do Paraná, Curitiba.

Zeng P., 1998. Composite element method for vibration analysis of structures, part I: principle and C^0 element (bar). *Journal of Sound and Vibration*. Vol. 218, n. 4, p. 619-658.